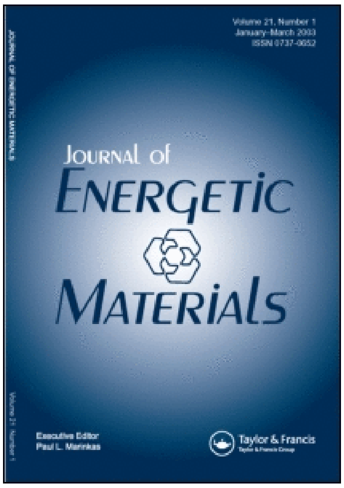

Journal of Energetic Materials
Publication details, including instructions for authors and subscription information:
http://www.informaworld.com/smpp/title~content=t713770432

High-pressure electrical resistance, optical, and structural studies of hmx and rdx during thermal decomposition

G. C. Vezzoli[a]; Yvon P. Carignan[a]
[a] U.S. Army Armament Research & Development & Engineering Center Picatinny Arsenal, Dover, NJ

To cite this Article Vezzoli, G. C. and Carignan, Yvon P.(1988) 'High-pressure electrical resistance, optical, and structural studies of hmx and rdx during thermal decomposition', Journal of Energetic Materials, 6: 1, 1 — 25
To link to this Article: DOI: 10.1080/07370658808017234
URL: http://dx.doi.org/10.1080/07370658808017234

HIGH-PRESSURE ELECTRICAL RESISTANCE, OPTICAL, AND STRUCTURAL STUDIES OF HMX AND RDX DURING THERMAL DECOMPOSITION

G. C. Vezzoli and Yvon P. Carignan

U.S. Army Armament Research & Development & Engineering Center

Picatinny Arsenal, Dover, NJ 07801-5001

ABSTRACT

High-pressure elevated-temperature Bridgman anvil studies of HMX and RDX indicate that during chemical decomposition (and perhaps melting) the electrical resistance rapidly decreases about three orders of magnitude, attains a minimum, and thereafter generally increases with increasing temperature. Pressure studies of these materials from about 10 to 40 kbar do not show a monotonic trend regarding the pressure dependence of the temperatures of most of the electrical anomalies, and this observation is attributed to complex kinetic behavior. A subtle resistance maximum often observed in RDX in the lower temperature ranges may also be related to the initiation of a decompositional or phase effect.

INTRODUCTION

The molecular structures of HMX and RDX are shown in Figure 1. HMX (high melting explosive) or 1,3,5,7-tetranitro-1,3,5,7-

Journal of Energetic Materials vol. 6, 001-025 (1988)

Published in 1988 by Dowden, Brodman & Devine, Inc.

tetraazacycloctane, and RDX (1,3,5-trinitrotetrahydro-s-triazine or cyclotrimethylenetrinitramine) are both explosives. The above structures are based on a ring molecule which is expected to undergo thermally-induced covalent bond scission. In HMX and RDX, the rings are independent and linked via Van der Waals and London forces.

In the present experiments, the intention of the work was to study pressure and temperature induced structural change such as polymorphism, melting, and decomposition. Previous high pressure work on the energetic materials tetrasulfur tetranitride and polysulfurnitride [1,2], as well as on metal carbonates [3,4] had shown that major electrical resistance changes accompany thermal decomposition at pressure. Thus, it was planned to study structural changes in HMX and RDX by monitoring electrical resistance and optical transmission vs temperature at a series of approximately constant pressures, and then to study the recovered products by x-ray diffraction and electron microscopy.

EXPERIMENTAL

This study was conducted through the use of a Bridgman anvil apparatus in conjunction with a mica gasket and four disk-and-stem copper electrical contacts. The equipment and sample assembly are described elsewhere [5,6], and are schematized in Figure 2A. The gasket starting thickness was about 0.015" to 0.020", and diameter to thickness ratios of about 20:1 to 25:1 were maintained in order to ensure relatively uniform pressure distribution across the anvil faces [5]. Samples consisted of polycrystalline RDX and HMX. The i.d. of the gasket was generally 0.10". The sample was prepressurized into the gasket hole, and then was sandwiched symmetrically between tungsten carbide compound anvils of face diameter either 0.375" or 0.500". Pressure was slowly raised on the apparatus gauge and was previously calibrated through the phase transformation of Hg, Bi, Ba, and Cs. Pressures are judged accurate to ± 5 - 10%. Temperatures were measured by a chromel-alumel thermocouple within a few mm of the side of the sample, and are accurate to ± 2°C. The thermocouple was shielded from the direct heat of the split furnace by insulation surrounding the tempered region of the anvils. Care was taken to also surround the thermocouple with a layer of insulation to prevent the thermocouple bead from shorting out the anvils. Voltage and current were continuously monitored as a function of increasing and decreasing temperature through the use of a simple d.c. circuit, a digital mutimeter, and a Brush chart recorder. Heating and cooling rates were about 2°C/min.

Optical transmission versus temperature experiments were performed at constant pressure utilizing a diamond high pressure cell. White light was transmitted through the lower diamond anvil and through the sample as well as upper diamond. A beam splitter then allowed half the beam to be incident on a Harco television camera feeding into an RCA television monitor. The other half of the beam was directed to an EG&G photomultiplier (model 585-00-60) connected to an EG&G radiometer indicator unit, the output of which was fed into the Y-channel of a Hewlett Packard X-Y recorder. The entire diamond cell was heated by a heat gun, and temperature was measured via a chromel-alumel thermocouple imbedded into a hole in the diamond cell frame and fed into the X-channel of the X-Y recorder. The experimental setup is shown in Figure 2B.

EXPERIMENTAL RESULTS

RDX

Typical chart recorder raw data for RDX are given in Figure 3 at 20 kbar and show a sharp decrease in resistance at about 316°C followed by a minimum resistance turning point at 320°C, with the resistance thereafter increasing as the temperature continues to increase. The increasing current is accompanied by decreasing voltage across the sample at constant applied voltage. Prior to the sharp increase in conductance, a satellite region or small secondary resistance minimum anomaly is observed. Another set of raw data for a high pressure are given in Figure 4 and plotted semilogarthmically as resistance vs temperature in Figure 5. In these data a shallow low-temperature turning point (resistance maximum) is observed near 212°C similar to what we often observe in nitrocellulose (to be published separately). Table 1 gives two sets of data for the temperatures of electrical anomalies during decomposition for various pressures and includes: T_o = shallow low temperature resistance maximum; T_b = temperature for the beginning of the resistance decrease region; T_1 = sharp current increase, T_2 = resistance minimum. Monotonic trends in $T_{anomaly}$ vs pressure are not apparent.

HMX

Electrical data during the decomposition of HMX are given in Figures 6-9. In this substance the decreasing resistance zone is generally very sharply defined (large increase in conductance) and occurs during a very small increase in temperature. The low temperature turning point (resistance maximum) which was observed in RDX is not detected in HMX. Figure 6 shows a further high temperature (344°C) turning point in resistance. Again, monotonic functional dependence of the temperatures of electrical anomalies vs pressure cannot be clearly extracted from the data; it can simply be concluded that changes in pressure do not seem to drastically change the temperatures of the electrical effects. In Figure 8 as temperature is being reduced, after the resistance minimum has been encountered, several plateau regions of current are observed as temperature continues to decrease. These regions may correspond to metastable or fairly short-lived species that are formed during the slow decomposition process or may possibly accompany a later reconstitution reaction. A semi-log plot of resistance vs temperature for HMX is given in Figure 9. Photographs of the starting material and those of the recovered product from an 11 kbar decomposition experiment are compared in Figures 10 and 11. Table 2A gives the anomaly temperatures (for increase in current, decrease in voltage, and minimum resistance) as a function of increasing pressure. Again, no specific trend is apparent. Table 2B gives the d-spacings and intensities for a recovered product from pressure-temperature treatment and compares these values to the x-ray powder pattern of the starting material.

DISCUSSION AND INTERPRETATION

The increase in conductance by several orders of magnitude during heating under pressure in HMX and RDX is believed to be due to stages of chemical decomposition. The conductance increase is probably an indication of the rapid scission of covalent bonds and the resulting presence of short diradically terminated chain segments. Electronic conduction can then take place at the unsatisfied valence spin sites by hopping. Ionic conduction can also occur via migration. During and after ring rupture, the outgassing of some chemical decomposition constituents such as NO_2 should occur. The Bridgman anvil cell does not form a hermetically tight seal to prevent the escape of gaseous molecules or atoms which have been released during the decompositional process. The diamond cell, using a stainless steel gasket or an inconel gasket, does, however, form a hermetic seal thereby retaining the gaseous molecules, or charged radicals. Thus, some of the electrical anomalies (such as T_v) may be attributable to loss of vapor species. These charged radicals should be influenced by an externally applied magnetic field to affect chemical reconstitution.

After the bond breaking process occurs, at sufficient temperature, a bonding reconstruction can take place whereby unsatisfied valence spins then tend to chemically unite and again close broken rings or lengthen chains, or cause cross linkage. The rebonding is expected to be associated with decreasing conductance since electrons that during the transitional state could be utilized for conductivity are now, during the end product stage, utilized for forming covalent bonds. This then may explain the resistance minimum as the conditions for the greatest concentration of diradical chain fragments at the appropriate kT.

The occasional observation in some of these materials of a maximum in electrical resistance at the lower temperature ranges of the experiment may be associated with the very initial stages of a chemical process or may on the other hand be associated with some physical process involving scattering and the molecular orbital energy band configuration of these materials. The effect is subtle and not totally reproducible but cannot be ignored.

The electrical resistance behavior vs temperature at pressure for HMX and RDX does not show the spiked conductance peaks observed in S_4N_4 during similar experiments.[1,2] The current peaks detected during the decomposition of S_4N_4 were attributed to the development of diradically terminated chain fragments created by the scission of the covalent ring molecule or bisphenoid. The nitrogen is then believed to be released and a sulfur chain molecule is formed. The latter does not conduct electrically, hence the high current state is only a transient. The S_4N_4 structure is composed of independent bisphenoids or ring-like molecules that in some way parallel octameric puckered sulfur rings (orthorhombic S_8). Hence we suspect that the species formed during the decomposition of RDX and HMX do not exist in short-lived transient states which would be associated with the molecular hybridization that establishes transient metallic behavior in a covalent material. Any transient states that may be associated with decompositions in HMX and RDX are too short lived to measure with the apparatus employed in this study. The sulfur-nitrogen chain or chain fragment that is formed from the broken bisphenoid has a unique molecular orbital configuration with delta and pi states creating unusual metallic behavior. In HMX and RDX any released NO_2 does not apparently cause transient phenomena, as the loss of nitrogen seems to cause in the sulfur-nitrogen system.

The observation that there does not seem to be a monotonic or systematic trend of temperatures for electrical anomalies vs pressure in RDX or HMX is thought to be attributable to very complex kinetic phenomena. Heating rate, cooling rate, microstructure, anvil surface, and i.d. gasket mechanical properties, can all influence the triggering conditions of a kinetically sensitive reaction such as decomposition in complex energetic materials. It is intended to perform a very systematic controlled kinetic study of these criteria in our next work on these materials. In an alternate study, the work of Block and

Piermarini[7] on RDX and HMX confirm the non-equilibrium and complex kinetic behavior of these materials.

REFERENCES

1. G. C. Vezzoli and J. Abel, Mat. Res. Bul. 13, 151 (1978).
2. G. C. Vezzoli and J. Abel, Science 200, 765 (1978).
3. G. C. Vezzoli and S. Krasner, High Temperatures - High Pressures 15, 27 (1983).
4. G. C. Vezzoli and S. Krasner, High Temperatures - High Pressures 15,41 (1983).
5. M. Myers, F. Dachille and R. Roy, Rev. Sci. Instrum. 34, 401 (1963).
6. G. C. Vezzoli, F. Dachille, and R. Roy, J. Amer. Ceram. Soc. 54, 221 (1971).
7. S. Block and G. Piermarini, Private Communication.

TABLE 1

Temperatures for Electrical Anomalies at Varying Pressures During Decomposition of RDX.

Series 1

Pressure (kbar)	T_o(°C)	T_b(°C)	T_1(°C)	T_2(°C)
2	---	302	306	320
3.5	162	218	225	244
7	---	266	---	---
10	---	266	307	343
16	---	256	290	blowout
21	182	295	312	320
28	184	330	329	355

Series 2

Pressure (kbar)	T_o(°C)	T_b(°C)	T_1(°C)	T_2(°C)
10	---	---	341	343
15	---	---	306	---
16	---	---	---	332
20	---	---	261	283
28	186	---	307	319
43	---	---	333	explosion

Temperatures: T_o = resistance maximum.

T_1 = sharply increasing current.

T_b = beginning of current increase.

T_2 = resistance minimum.

TABLE 2A

Temperatures for Electrical Anomalies at Varying Pressures During Decomposition of HMX.

Pressure (kbar)	T_o(°C)	T_1(°C)	T_v(°C)	T_2(°C)
9	---	319	343	343
11	---	355	365	369
13	---	355	367	360
21	---	357	---	369
22	---	402	414	414
27	---	343	355	355
42	---	403	---	---

Temperatures: T_o = resistance maximum.
T_1 = sharply increasing current.
T_v = sharply decreasing voltage across sample.
T_2 = resistance minimum.

TABLE 2B

X-Ray Diffraction Data for Starting HMX and for Decomposition Product Recovered from High P-T: (Debye Scherrer Data)

	HMX Starting Material		Decomposition Product	
	d(Å)	I	d(Å)	I
1.	6.10	S		
2.	5.57	S		
3.	4.82	M		
4.	4.33	S		
5.	4.09	W		
6.	3.86	S		
7.	3.62	VW		
8.	3.45	S		
9.	3.29	S		
10.	3.04	S	3.05	W
11.	2.80	S	2.77	MW
12.	2.70	W		
13.	2.53	W	2.56	S
14.	2.43	S	2.38	MW
15.	2.27	W	2.32	W
16.	2.18	M-S		
17.	2.13	M-S	2.14	MW
18.	2.08	M-W		
19.	2.02	M	2.02	W
20.	1.99	M	1.96	VVW

TABLE 2B--PAGE 2

X-Ray Diffraction Data for Starting HMX and for Decomposition Product Recovered from High P-T: (Debye Scherrer Data)

	HMX Starting Material		Decomposition Product	
	d(Å)	I	d(Å)	I
21.	1.90	M		
22.	1.87	M	1.84	VW
23.	1.80	S		
24.	1.74	W	1.74	VW
25.	1.66	W	1.71	VVW
			1.66	M
26.	1.46	W	1.61	VVW
27.	1.39	W	1.56	VVW
			1.50	M
28.	1.35	W	1.49	W
			1.36	W
29.	1.31	W	1.34	W
30.	1.27	MW	1.29	VW
31.	1.21	MW	1.24	W
32.	1.18	VW		

S-Strong; M-Medium; W-Weak; V-Very

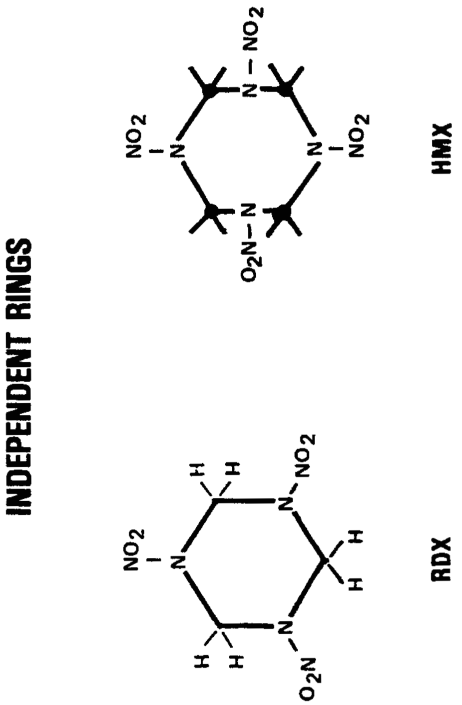

Figure 1. The molecular structure of RDX and HMX.

SAMPLE ASSEMBLY FOR HIGH PRESSURE FOUR-TERMINAL ELECTRICAL RESISTANCE MEASUREMENTS

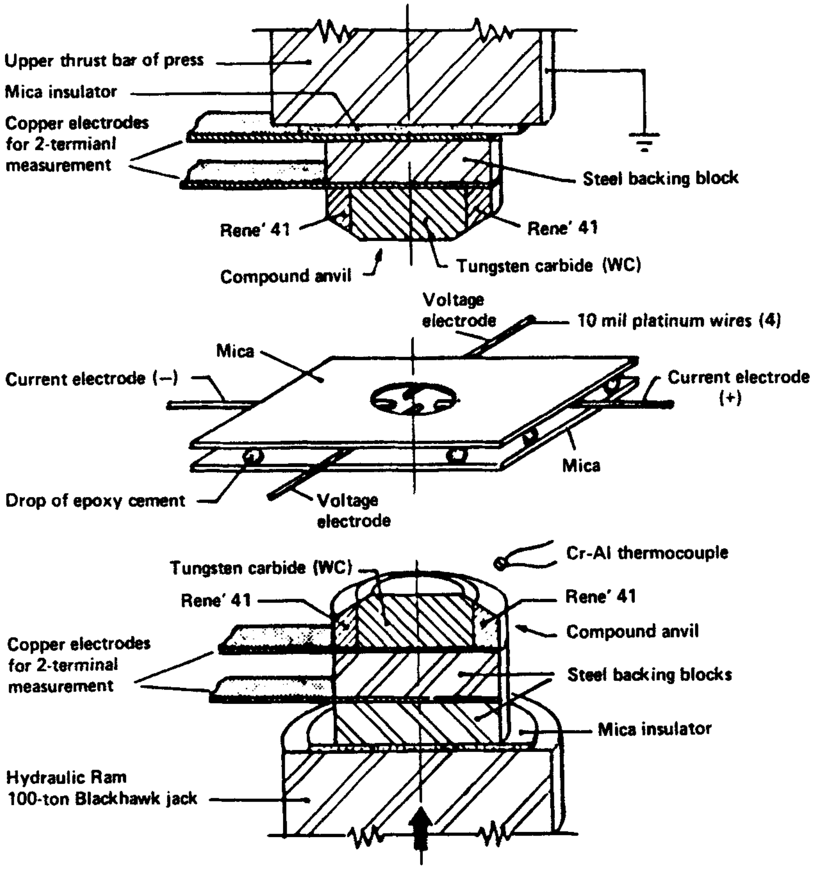

Figure 2A. Schematic of high pressure Bridgman anvil apparatus.

SCHEMATIC OF APPARATUS FOR MEASURING OPTICAL TRANSMISSION vs TEMPERATURE AT PRESSURE USING DIAMOND CELL

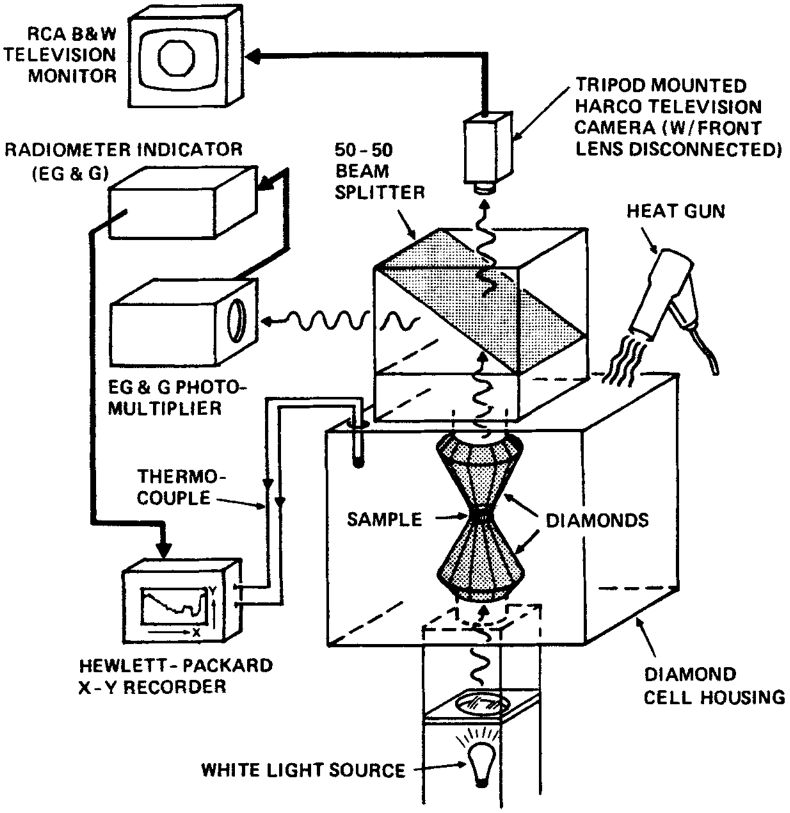

2B. Schematic of setup for measuring optical transmission vs temperature at pressure (diamond cell).

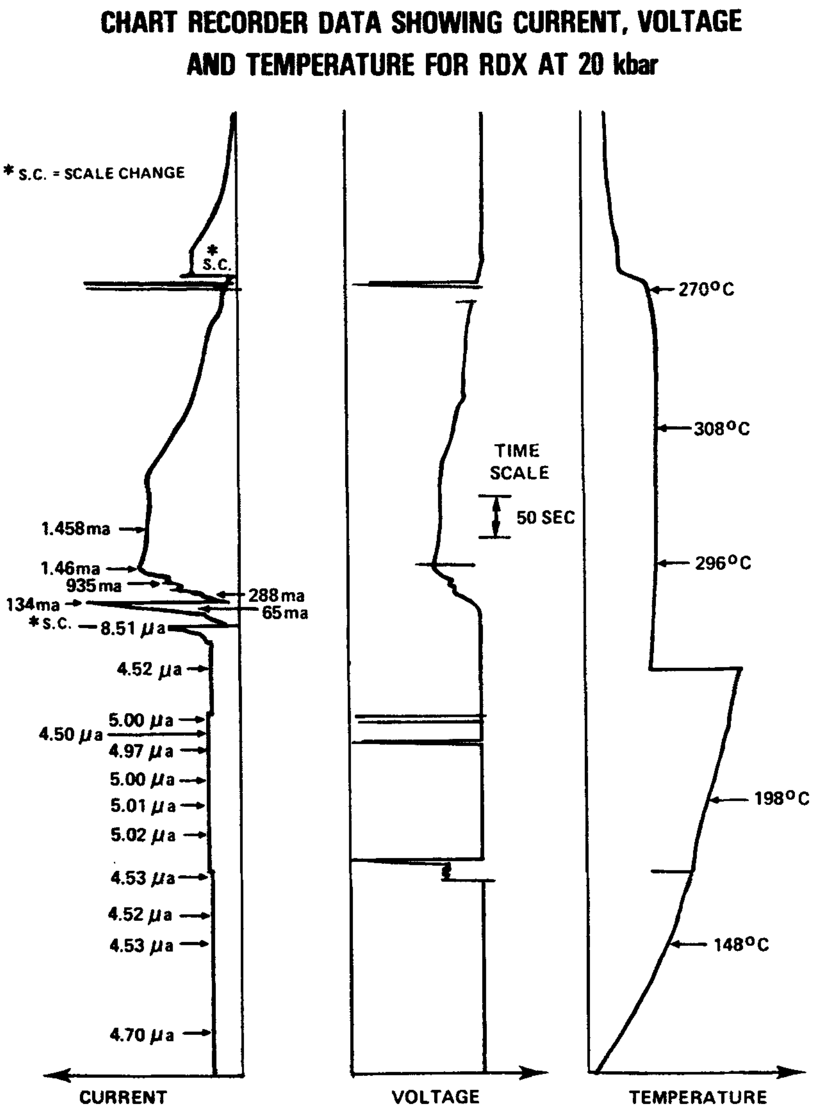

Figure 3. Raw chart recorder data during decomposition of RDX at 20 kbar giving current, voltage across sample and temperature.

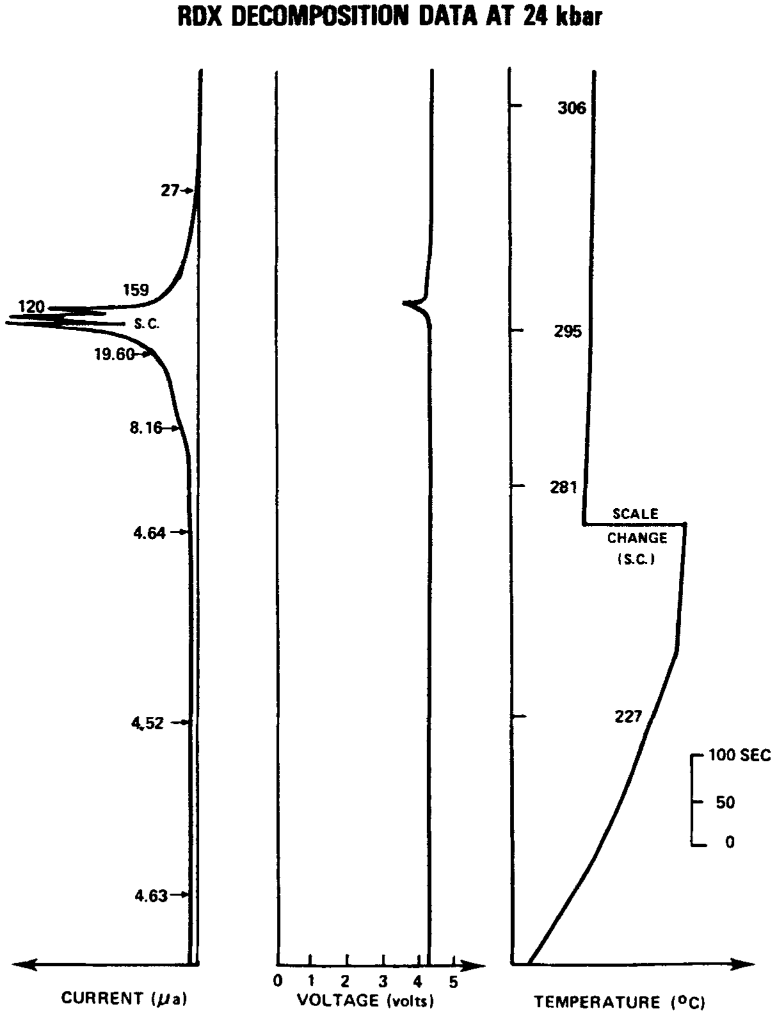

Figure 4. Raw chart recorder data during decomposition of RDX at 24 kbar.

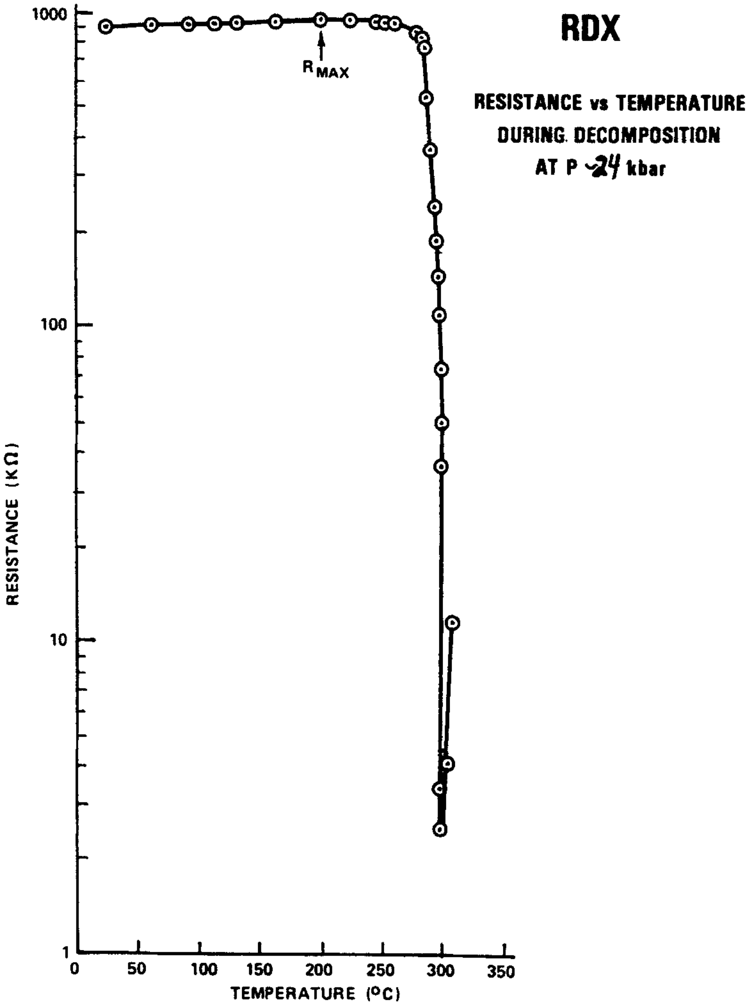

Figure 5. Semilog plot of resistance vs temperature for data from Figure 4.

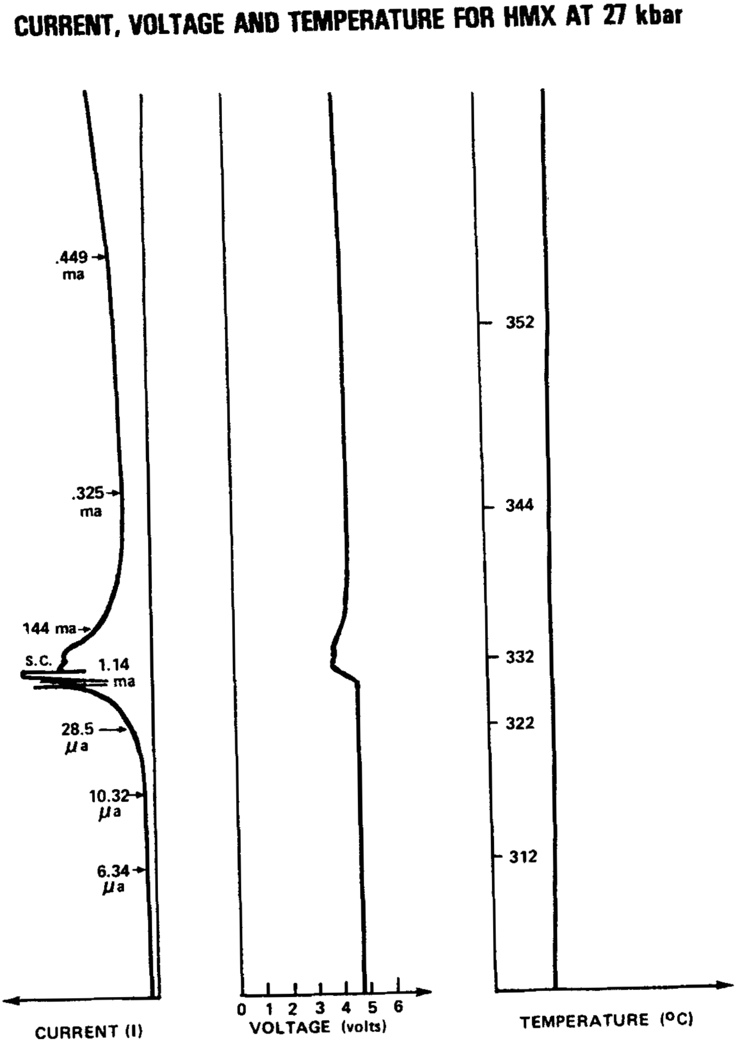

Figure 6. Raw chart recorder data during decomposition of HMX at 27 kbar.

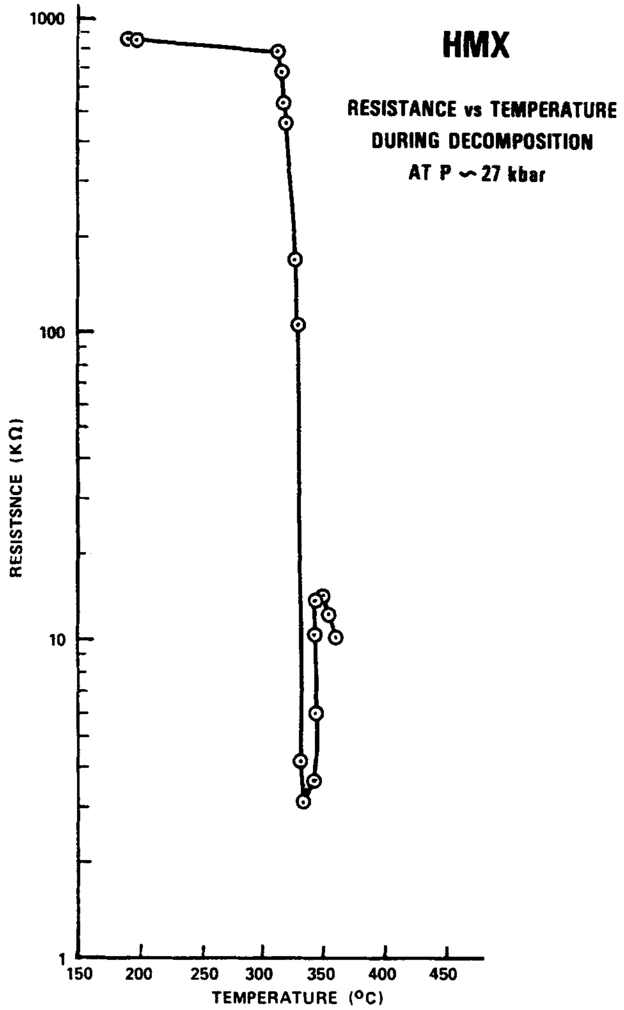

Figure 7. Semilog plot of electrical resistance vs temperature for data from Figure 6.

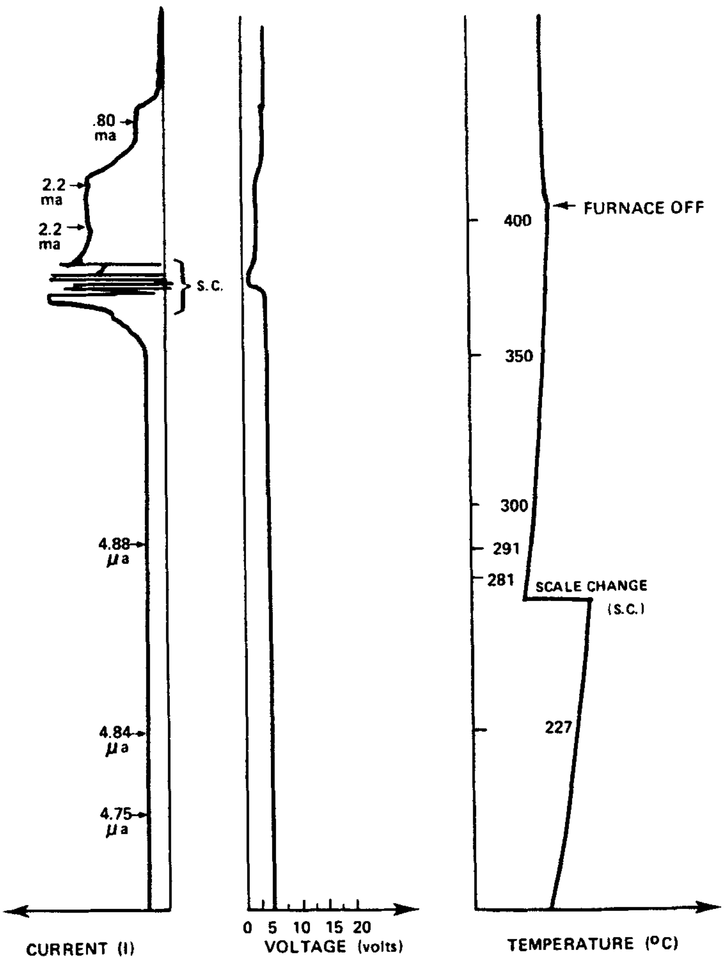

HMX DECOMPOSITION DATA AT 16 kbar

Figure 8. Raw chart recorder data during decomposition of HMX at 16 kbar. Note plateau regions in current.

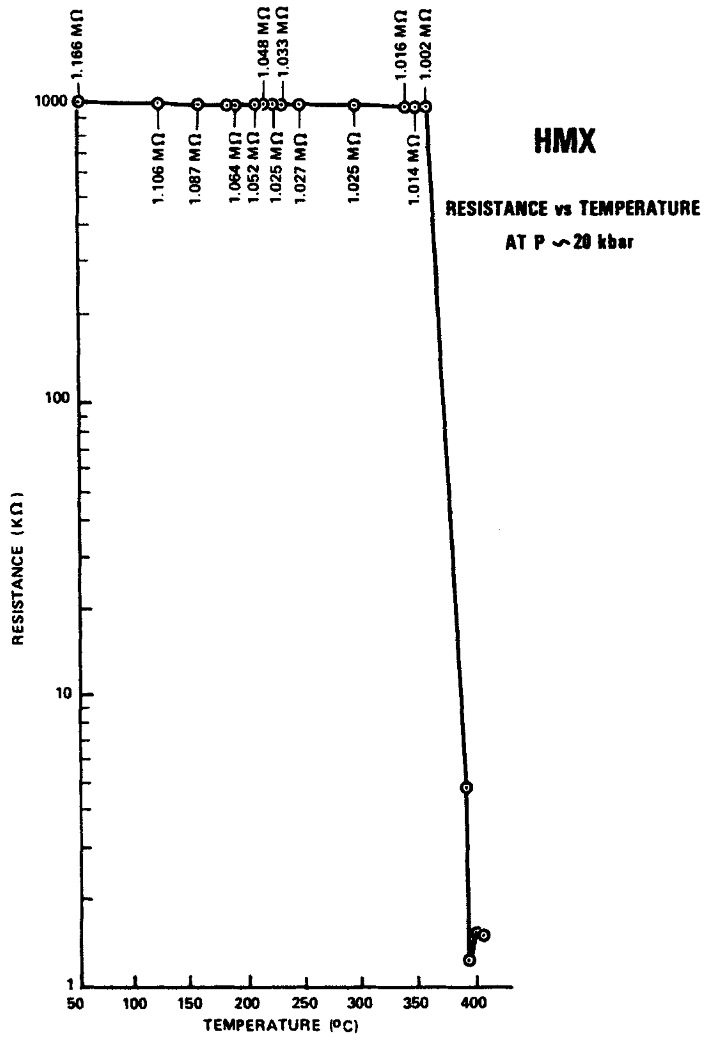

Figure 9. Semilog plot of electrical resistance vs temperature for data from Figure 8.

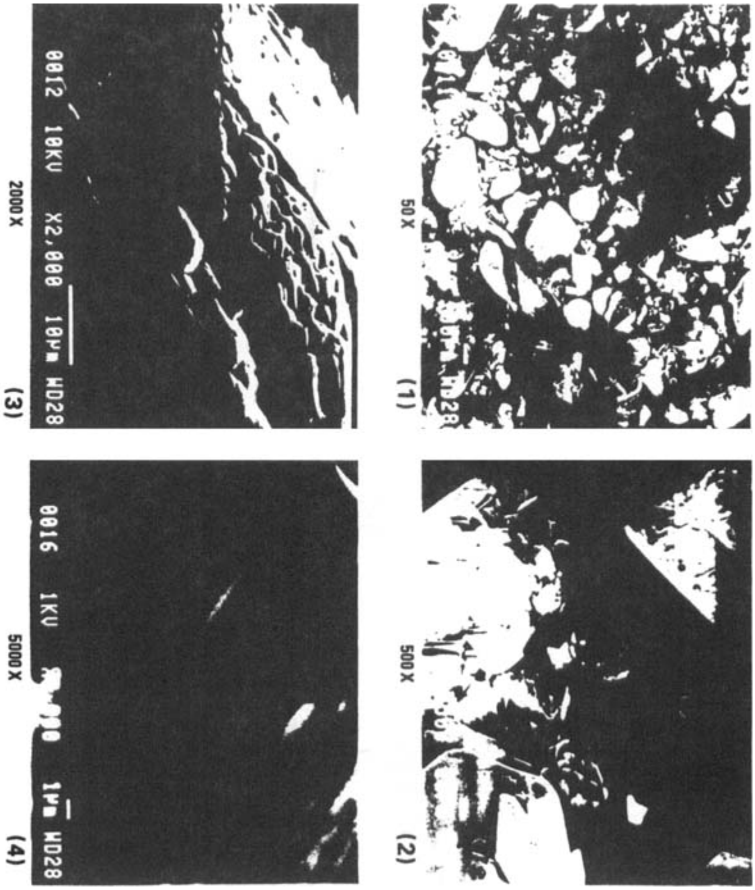

SCANNING ELECTRON MICROSCOPE PHOTOGRAPHS OF HMX STARTING MATERIAL (POLYCRYSTALLINE)

Figure 10. Scanning electron microscope photographs of starting material HMX.

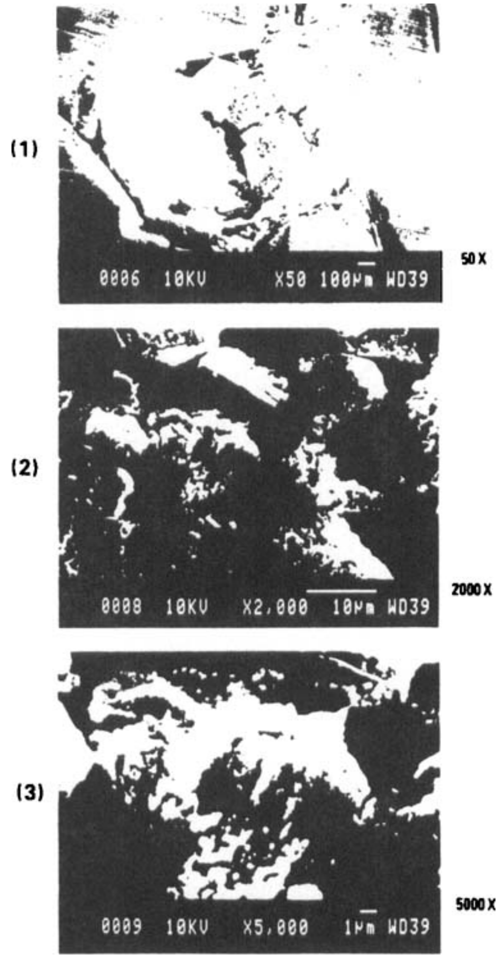

SCANNING ELECTRON MICROSCOPE PHOTOGRAPHS OF RECOVERED PRODUCT

(FROM 11 kbar AT 300°C, USING POLYCRYSTALLINE HMX STARTING MATERIAL)

Figure 11. Scanning electron microscope photograph of recovered product from 11 kbar at elevated temperature using HMX starting material.